

G. Perentzis · E. Horopanitis · I. Samaras  
S. Kokkou · L. Papadimitriou

## Synthesis and electrochemical study of Li-Mn-Ni-O cathodes for lithium battery applications

Received: 15 November 2002 / Accepted: 11 June 2003 / Published online: 12 August 2003  
© Springer-Verlag 2003

**Abstract** Cathode powders of the Li–Mn–Ni–O system have been prepared at a  $Mn/(Mn + Ni)$  ratio varying from 0 to 1. The solid state reaction method was used to obtain the cathode materials by mixing  $MnO_2$ ,  $LiCO_3$  and NiO. A 20% excess of lithium was used in the precursors. The materials produced were examined by X-rays to identify their structure. Batteries were assembled by using these materials as cathode with a liquid electrolyte consisting of EC/DMC 1:1, 1M  $LiPF_6$  and Li anode. Their capacity, cycle fading and charge-discharge conditions were evaluated.

**Keywords** Solid state reaction · Lithium battery · Lithium · Manganese · Nickel · Cathode

### Introduction

Spinel  $LiMn_2O_4$  is one of the most important materials for use in rechargeable lithium ion batteries. It is well known that 2 lithium ions can be intercalated reversibly in the spinel at 4 and 3 V respectively. The capacity of the material is 140 mAh/g for the 4 V region and reaches 308 mAh/g when cycled down to 3 V [1]. Low cost and its environmental properties, which include lower toxicity compared to other candidate materials (mainly cobalt and nickel oxides) make manganese oxide an attractive solution for application in lithium ion bulk

and thin film batteries. However, the biggest disadvantage is its poor cycling behavior compared to  $LiCoO_2$ . The insertion of more than one lithium per mole in the structure induces a Jahn-Teller distortion in the spinel reducing it from cubic  $Fd3m$  to tetragonal symmetry. This distortion results in a capacity fade when deeply discharging and recharging the battery [2]. Partial substitution of Mn with other transition metals (Ni, Co) show an improved cyclability at the expense though of the initial capacity of the material, at least in the 4.1 V plateau.

By increasing the percentage of Ni in order to replace Mn the R3m structure in the material appears, which consists of a close-packed oxygen atoms array with lithium and nickel atoms filling alternate layers.  $LiNiO_2$ , which is finally obtained by 100% substitution of Mn with Ni, is another transition metal oxide which is intensively studied for its potential use as a cathode material in lithium ion batteries. However, it is difficult to fully oxidize  $Ni^{2+}$  to  $Ni^{3+}$ . Therefore, a lithium deficient  $Li_{(1-z)}Ni_{(1+z)}O_2$  non-stoichiometric oxide is synthesized. Efforts have been made in order to improve the stability of the material, when fully charged [3, 4], by trying different synthesis methods and conditions. Divalent nickel ion insertion into lithium sites [5] has been identified as the main reason for the non-stoichiometric material because of the stable environment for the  $Ni^{2+}$  in these sites.  $LiNiO_2$  has a high specific capacity of 276 mAh/g for a one lithium atom insertion per formula, which is delivered between 3.5 and 4.7 V. Nevertheless, cycling between 3.5 and 4.1 V (0.5 Li per formula) has shown a capacity of 135 mAh/g, which is more cycleable than a fully charged battery [6].

Presented at the 3rd International Meeting “Advanced Batteries and Accumulators”, June 16th–June 20th 2002, Brno, Czech Republic

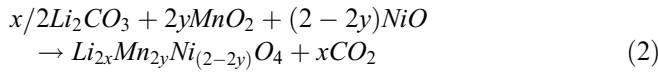
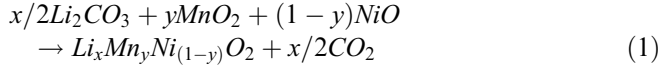
G. Perentzis · E. Horopanitis · I. Samaras · L. Papadimitriou (✉)  
Section of Solid State Physics, Department of Physics,  
Aristotle University of Thessaloniki, Greece  
E-mail: pleonida@auth.gr  
Tel.: 998 214

S. Kokkou  
Section of Applied Physics, Department of Physics,  
Aristotle University of Thessaloniki, Greece

### Synthesis

Cathode materials of the Li–Mn–Ni–O system have been prepared by using the solid state reaction method while staying at an elevated temperature for a specific time.  $MnO_2$  (Aldrich), NiO (Aldrich), and  $Li_2CO_3$

(Aldrich) are used as starting materials for all synthesised powders. The material quantities used in the initial mixing were decided according to the following chemical equations:



The ratio  $\frac{\text{Li}}{(\text{Ni} + \text{Mn})}$  is 1.2 for all preparations. Since the products of these equations are either a spinel, cubic phase or a rhomboedral material, the choice of the ratio  $\text{Mn}/(\text{Mn} + \text{Ni})$  is crucial in order to use the right equation to produce the oxides. The phase of the materials was decided according to the bibliography and verified with XRD measurements. Heating at a desired temperature  $T_1$  followed in a Thermal Technology TL1350 furnace. The powders remained in the furnace in an alumina crucible for 19–21 h and they were removed in order to grind the solid that was formed. After being ground, the materials are reinserted in the furnace at a temperature  $T_2$ , followed by a slow cooling in  $\text{O}_2$  atmosphere. Synthesis conditions of the materials are presented in Table 1.

## Experimental

The synthesized materials were characterized by XRD and their structure was verified. Pills were fabricated from the powders in order to use them as cathode electrodes in electrochemical measurements. Acetylene black was added in order to improve conductivity. Polyvinylidene fluoride binder, PvdF (Aldrich), diluted in cyclopentanone (Fluka), was used as a stabilizer in some of the pills as shown in Table 2. Cathode material, acetylene black, and PvdF, after having being well mixed, producing a slurry when PvdF was present, were spread on a round aluminium substrate (diameter of 12 mm) and left to dry at 120 °C. The aluminum substrate also serves as an ohmic contact. Dried electrodes were consequently pressed under 7 tons of pressure to produce pills, which were then heated at 120–180 °C for 30 min and were placed into stainless steel cells in order to evaluate their electrochemical properties. On top of the cathode material a microporous glass fiber separator was positioned, impregnated with 1 M LiPF<sub>6</sub> electrolyte in a 1:1 solution of ethylene carbonate and dimethyl-carbonate. Lithium foil served as the anode material. The fabrication of the cells took place in an argon-filled glove box.

**Table 1** Conditions of synthesis

Sample code	Chemical formula	$T_1$ (°C)	$t_1$ (h)	$T_2$ (°C)	$t_2$ (h)	Cooling (h)
GM20_12	$\text{Li}_{1.2}\text{Mn}_2\text{O}_4$	750	21	750	72	10
GO75_17	$\text{Li}_{1.2}\text{Mn}_{1.5}\text{Ni}_{0.5}\text{O}_4$	750	21	750	72	10
GO60_16	$\text{Li}_{1.2}\text{Mn}_{0.6}\text{Ni}_{0.4}\text{O}_2$	750	21	750	72	10
GO50_10	$\text{Li}_{1.2}\text{Mn}_{0.5}\text{Ni}_{0.5}\text{O}_2$	750	19	750	66	24
GO25_11	$\text{Li}_{1.2}\text{Mn}_{0.25}\text{Ni}_{0.75}\text{O}_2$	750	19	750	66	24
GO20_15	$\text{Li}_{1.2}\text{Mn}_{0.2}\text{Ni}_{0.8}\text{O}_2$	750	19	750	72	10
GN20_18A	$\text{Li}_{1.2}\text{NiO}_2$	750	21	750	1	13
GO25_20*	$\text{Li}_{1.2}\text{Mn}_{0.25}\text{Ni}_{0.75}\text{O}_2$	750	21	750	72	10

The electrochemical measurements were conducted with an potentiostat/galvanostat Arbin Instruments which can drive up to 32 channels simultaneously. The cells were cycled galvanostatically in a potential range of 3.0 to 4.85 V, depending on the material and its XRD characterization. The current density was usually 55  $\mu\text{A}/\text{cm}^2$  unless explicitly stated in Table 3.

## Results and discussion

XRD diagrams in Fig. 1 show a good agreement between spinel  $\text{LiMn}_2\text{O}_4$  synthesized in our laboratory and typical spinels in recent publications [7]. The lattice constant,  $a$ , of our material is 8.228635 Å, almost equal to 8.223 Å which is given for high temperature synthesized  $\text{LiMn}_2\text{O}_4$  [7]. When nickel is used to substitute manganese the structure initially remains cubic but the rhombohedral system R3m appears at higher concentration of Ni. For ratio of  $\text{Mn}/(\text{Mn} + \text{Ni}) = 75\%$  the system remains mainly cubic, while lattice constant slightly diminishes to 8.1679 Å, as expected [3]. When  $\text{Mn}/(\text{Mn} + \text{Ni}) < 60\%$  the main structure identified is rhombohedral of the layered type  $\alpha\text{-NaFeO}_2$ . However, a second phase is observed, the monoclinic C2/c, which can be attributed to the growth of  $\text{Li}_2\text{NiO}_3$ , as described by Neudecker et al [8] for  $\text{Li}/(\text{Mn} + \text{Ni}) > 1.15$ . Rhombohedral phase material exists on its own when  $\text{Mn}/(\text{Mn} + \text{Ni}) \leq 25\%$  is reached with  $c = 14.25935$  Å and  $a = 2.898778$  Å. The lattice constant,  $a$ , decreases with Mn content.

Electrochemical measurements were performed on the pills and their results are shown in Table 3. Pills with acetylene black and PvdF perform better in terms of initial delivered capacity, when the voltage range is taken into account, and cycling performance except for ratios  $\text{Mn}/(\text{Mn} + \text{Ni}) = 50\%$  and 25%, for which no such pills were prepared.

Comparing the results for initial discharge capacity, it is clear that materials closer to the extreme concentration, either of Ni or Mn, perform better than those in the range  $75\% \leq \frac{\text{Mn}}{\text{Ni} + \text{Mn}} \leq 50\%$ . The latter, when cycled between 3.0 and 4.4 V, exhibit a very low discharge

**Table 2** Pills used in electrochemical measurements

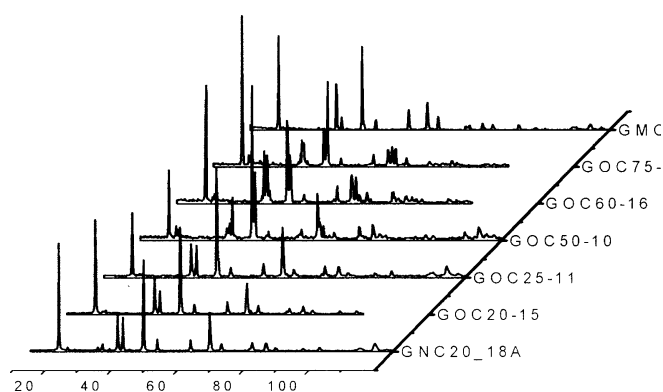
Code	Powder material	Material weight (mg)	Acetylene black (mg)	PvdF (mg)
GM12_2	$\text{Li}_{1.2}\text{Mn}_2\text{O}_4$	15.8		
PM12_2	$\text{Li}_{1.2}\text{Mn}_2\text{O}_4$	11.2	0.9	
GO17_1	$\text{Li}_{1.2}\text{Mn}_{1.5}\text{Ni}_{0.5}\text{O}_4$	27.7		
PO17_3	$\text{Li}_{1.2}\text{Mn}_{1.5}\text{Ni}_{0.5}\text{O}_4$	13.9	1.7	0.9
PO17_4	$\text{Li}_{1.2}\text{Mn}_{1.5}\text{Ni}_{0.5}\text{O}_4$	21.4	2.5	1
PO16_1	$\text{Li}_{1.2}\text{Mn}_{0.6}\text{Ni}_{0.4}\text{O}_2$	13.3		
PO16_3	$\text{Li}_{1.2}\text{Mn}_{0.6}\text{Ni}_{0.4}\text{O}_2$	14.1	1.8	1
PO10_3	$\text{Li}_{1.2}\text{Mn}_{0.5}\text{Ni}_{0.5}\text{O}_2$	12.5		
GO11_4	$\text{Li}_{1.2}\text{Mn}_{0.25}\text{Ni}_{0.75}\text{O}_2$	47.1		
GO15_2	$\text{Li}_{1.2}\text{Mn}_{0.2}\text{Ni}_{0.8}\text{O}_2$	29.4		
PO20_2	$\text{Li}_{1.2}\text{Mn}_{0.2}\text{Ni}_{0.8}\text{O}_2$	11.7	1	0.8
PN18A_1	$\text{Li}_{1.2}\text{NiO}_2$	15.5	0.8	1.1
PN18AG_3	$\text{Li}_{1.2}\text{NiO}_2$	14.1	1.8	0.8

**Table 3** Electrochemical measurements of cathode materials

	Material	Specific capacity (mAh/g)	Voltage range (V)	Capacity retention(% at number of cycles)	Theoretical specific capacity for 1 Li insertion(%)
*GM12_2	$\text{Li}_{1.2}\text{Mn}_2\text{O}_4$	79.65	3.2–4.5	46% at 10	66.40
PM12_2	$\text{Li}_{1.2}\text{Mn}_2\text{O}_4$	114.78	3.0–4.4	69% at 10	81.00
GO17_1	$\text{Li}_{1.2}\text{Mn}_{1.5}\text{Ni}_{0.5}\text{O}_4$	11.88	3.0–4.5	n/a	8.47
PO17_3	$\text{Li}_{1.2}\text{Mn}_{1.5}\text{Ni}_{0.5}\text{O}_4$	9.89	3.2–4.3	66% at 20	7.05
		24.85	3.2–4.7	78% at 30	17.71
PO17_4	$\text{Li}_{1.2}\text{Mn}_{1.5}\text{Ni}_{0.5}\text{O}_4$	37.6	3.2–4.8	72% at 20	26.80
PO16_1	$\text{Li}_{1.2}\text{Mn}_{0.6}\text{Ni}_{0.4}\text{O}_2$	19.47	3.0–4.4	n/a	7.54
PO16_3	$\text{Li}_{1.2}\text{Mn}_{0.6}\text{Ni}_{0.4}\text{O}_2$	16.59	3.5–4.3	88% at 50	6.42
		61.43	3.5–4.85	102% at 20	23.77
PO10_3	$\text{Li}_{1.2}\text{Mn}_{0.5}\text{Ni}_{0.5}\text{O}_2$	4.74	3.0–4.4	n/a	1.83
GO11_4	$\text{Li}_{1.2}\text{Mn}_{0.25}\text{Ni}_{0.75}\text{O}_2$	80.35	3.0–4.4	n/a	31.48
*GO15_2	$\text{Li}_{1.2}\text{Mn}_{0.2}\text{Ni}_{0.8}\text{O}_2$	100.24	3.0–4.4	87% at 5	39.5
PO20_2	$\text{Li}_{1.2}\text{Mn}_{0.2}\text{Ni}_{0.8}\text{O}_2$	102.32	3.5–4.3	91.5% at 5	40.17
PN18A_1	$\text{Li}_{1.2}\text{NiO}_2$	120.76	3.2–4.5	n/a	47.5
**PN18AG_3	$\text{Li}_{1.2}\text{NiO}_2$	90.68	3.5–4.3	67% at 10	35.85

\*Measurements performed at  $100 \mu\text{A}/\text{cm}^2$

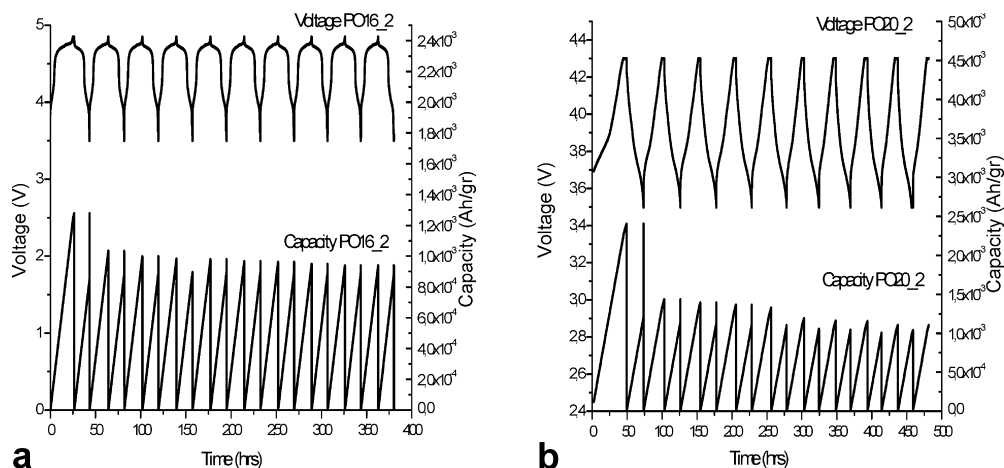
\*\*Ground before pill

**Fig. 1** X-ray patterns of prepared powder samples

capacity. In recent bibliography [3] it is shown that such materials can have a considerable discharge capacity stored at a higher voltage vs Li, thus we cycled the same cells between 3.5–4.85 V. It was confirmed that there are two plateaus at 4.72 and 4.76 V for  $Mn/(Mn + Ni) = 60\%$  and  $75\%$ . Capacity retention was very good for these materials even when cycled up to 4.8 V,

as shown in Fig. 2a. However, their capacity was still low compared to the theoretical capacity for 1 Li insertion into such a material which can be attributed to the coexistence of two phases. Materials within this range may perform better if produced as single phase and this is under investigation.  $\text{LiMn}_2\text{O}_4$  pills reach quite near to their theoretical capacity and show good retention of capacity considering that no binding material was used in either of these. Pure  $\text{LiNiO}_2$  show a high specific capacity, especially when taken into account that they are cycled only in the range 3.5–4.3 V. In our opinion, the material that was ground before forming the pill performs better in even smaller range of voltages although its cycling behavior is typical of the material and deteriorates quickly. Substitution of 20% nickel atoms to manganese improves the overall qualities of the material especially when cycled between 3.5–4.4 V (Fig. 2b).

The shape of the voltage curve is shown in Fig. 3 for some of the materials used for electrochemical measurements. For  $\text{LiMn}_2\text{O}_4$  in Fig. 3a, it is easy to distinguish the plateaus at 4 and 4.16 V. The former is due to the coexistence of the two distinct phases  $\text{LiMn}_2\text{O}_4$  and

**Fig. 2 a** e/c measurement of PO16\_3. **b.** e/c measurement of PO20\_2

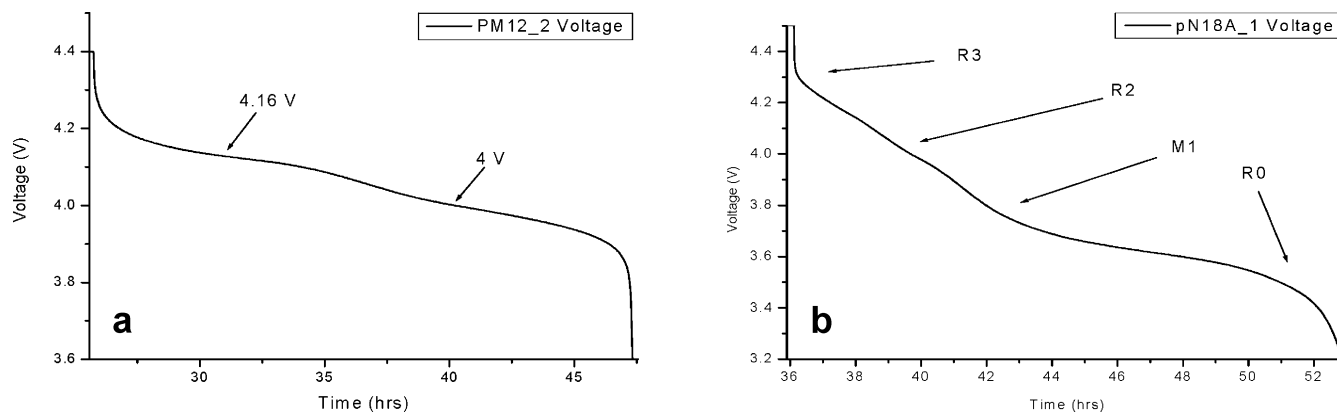


**Fig. 3** a Discharge curve of PM12\_2. b. Discharge curve of PN18A\_1

$\text{Li}_{0.5}\text{Mn}_2\text{O}_4$ , while the latter exists because of  $\text{Li}_{0.5}\text{Mn}_2\text{O}_4$  and  $\lambda\text{-MnO}_2$  [9]. In Fig. 3b, showing the discharge curve for  $\text{LiNiO}_2$ , four phases can be found. These are R1 (rhombohedral), M1 (monoclinic), R2 (rhombohedral) [10] and R3 (rhombohedral). The transition from R1 to M1 is reversible, which is not the case for the transition from R2 to R3. This happens because when  $\text{Ni}^{2+}$ , which are found in lithium sites in the lattice, are fully oxidized the distance between NiO layers decreases and intercalation of lithium ions is thus prohibited when discharging [6]. The existence of  $\text{Ni}^{2+}$  ions in the lattice is not incompatible with lithium abundance during synthesis of the material, according to Delmas [4]. Sample PN18A\_1 was measured in the range 3.2–4.5 V which includes the R2 to R3 transition, and we believe this is the reason for the poor cycling behavior of this pill. On the contrary, PN18AG\_1 exhibits a much better cycling performance most probably because of being cycled only up to 4.3 V. Sample PO20\_2 exhibited a similar to  $\text{LiNiO}_2$  discharge curve, although the plateaus at the same voltage values were smaller, which leads us to conclude that similar phase transformation take place in this material. However, its better cycling behavior shows that this material is a better candidate for cathode, if optimized.

## Conclusions

Substitution of nickel with manganese in lithiated transition metal oxides is an interesting alternative for a cathode material. The solid state synthesis method, for different  $Mn/(Mn + Ni)$  ratios, revealed that materials prepared in this way have a different structure depending on this ratio. All of them have an interesting electrochemical behavior but we would like to focus on the good capacity retention and the possible structural features of the samples with  $Mn/(Mn + Ni)$  75%, 60%, 20%.

**Acknowledgements** This work was funded by the NATO Science for Peace research project Sfp972523, “Li-ion rechargeable microbatteries integrable on low power ICs”.

## References

1. Amine K et al (1997) J Power Sources 68:604
2. Huang H et al (2000) Solid State Ionics 127:31
3. Zhong Q et al (1997) J. Electrochem Soc 144:205
4. Delmas C et al (1999) Electrochim Acta 45:243
5. Spahr M et al (1997) J Power Sources 68:629
6. Guyomard D (2000) In: Osaka T, Datta M (eds) Energy storage systems for electronics. Gordon and Breach, Amsterdam
7. Nitta Y et al (1997) J Power Sources 68:166
8. Neudecker BJ et al (1998) J Electrochem Soc 145:4148
9. Sun Y et al (1999) J Power Sources 79:231
10. Croguennec L et al (2000) J Electrochem Soc 147:1314